Chapter 18

Selected Solar Influences on the Magnetosphere: Information from Cosmic Rays

Karel Kudela and Leonid L. Lazutin

Abstract The state of the magnetosphere is influenced by the effects driven from the solar surface. The models of geomagnetic field are parametrized by the magnetopshere activity indices which are related to IMF and solar wind characteristics. Cosmic rays could serve as a tool for "remote sensing" of the redistribution of IMF structure in interplanetary space and for checking validity of geomagnetic field models with external current systems. The anisotropy of cosmic rays observed on the ground is influenced by superposition of (a) interplanetary anisotropy due to transitional effects and by (b) variable transmissivity of magnetosphere itself. The possibilities to deconvolute the two dependences is discussed. Anisotropy observed at neutron monitors and muon telescopes just before the onset of some geomagnetic storms is reviewed. The changes of geomagnetic cut-off, structure of the transmissivity function and asymptotic directions for various geomagnetic field models during strong geomagnetic storms are discussed. Low altitude polar orbiting satellites with large geometric factors for high energy particles (e.g. CORONAS-F) are suitable for (a) estimates of energy spectra of solar or interplanetary accelerated particles by checking the outer zone boundary of trapping and for (b) checking how the different geomagnetic field models are fitting the observed trapped particle profiles in different local time sectors. Independently on the state of magnetosphere, the measurements of energetic "neutral emissions" (gammas and neutrons) near the Earth or on the ground, serve as indicator of acceleration processes on solar surface.

18.1 Introduction – Cosmic Rays and Space Weather

Cosmic rays including the particles accelerated to high energy in solar flares or at the CMEs are affecting the magnetosphere especially at high latitudes and the atmosphere at high altitudes. The onset of high energy particle flux at the Earth is the first indication of possible radiation hazard storm near the Earth. The cosmic ray (CR) anisotropy observed by the ground based stations can serve as one of the elements of the alert before the geoeffective events. The book by Dorman (2009) provides a comprehensive review of the cosmic ray interaction with the magnetosphere. The relations of the cosmic ray studies to the space weather effects are reviewed e.g. in Kudela et al. (2000); Kudela (2009) among the other papers.

18.1.1 Short Time Forecast of Radiation Storms

The particles with the energy of several tens to hundreds of MeV are the most important for the radiation hazard effects during solar radiation storms with the electronic element failures on satellites, communication and with biological consequences. Before their massive arrival, the detectors of the CRs observing secondaries above the atmospheric threshold and at locations with various cutoff rigidity can provide useful alerts several minutes to tens minutes in advance, if the good temporal resolution and network by many stations is in real time operation. The neutron monitor (NM) at single site (high latitude,

K. Kudela (✉)
IEP SAS, Watsonova 47, 040 01 Kosice, Slovakia
e-mail: kkudela@upjs.sk

good statistics) allows to obtain a real time energy spectrum. For January 20, 2005 event it was shown at the South Pole by combination of NM64 and by that lacking usual lead shielding (Bieber et al. 2006). The ground level enhancement (GLE) real-time alarm based on the 8 high latitude NMs including those at high mountain is described in the paper Kuwabara et al. (2006). A three level alarm system (by number of NMs exceeding threshold value above that of the baseline) is suggested. Out of 10 GLEs in 2001–2005 archived data the system produced 9 correct alarms. The GLE system gives earlier warning than the satellite (SEC/NOAA) alert. Recently the paper by Su et al. (2009) checked the potential of the South Pole NM data and the data from monitor lacking the shielding for prediction of radiation storm intensity measured by the GOES. The data from the two groups of the GLE used (12 compared with P4–P8, 7 additionally compared with high energy channels of the GOES) have shown that the South Pole GLE observations can be used to predict radiation intensity of the higher energy proton channels from the GOES.

Recently, also the progress in using the NM at low and middle latitudes is reported before the radiation storms. Several steps of the GLE alert algorithm using the NM network have been described by Mavromichalaki et al. (2009) in the NMDB project (http://www.nmdb.eu).

The paper by Anashin et al. (2009) describes another type of alert signal for GLEs which can be found in real time at http://cr0.izmiran.ru/GLE-AlertAndProfiles and forecast of Solar Neutron Alert at: http://cr0.izmiran.ru/SolarNeutronMonitoring.

In addition to the early GLE alerts by the ground based NMs the forecasts from satellite data are reported. The paper by Posner (2007) demonstrates the important possibility of short-term forecasting of the appearance and intensity of solar ion events by means of relativistic electrons measured on satellites.

When high energy particles strike the atmosphere, they produce the secondary population (and the tertiary one in the NMs) and change the ionisation and contribute to the dose at airplane altitudes and above. The longest data set of ionizing component of secondaries at different altitudes has been collected in FIAN Moscow (Stozhkov et al. 2007). While the ionization measured by Geiger counters has strong solar activity

cycle variation at high altitudes, it is not the case for low altitudes (Bazilevskaya et al. 2008). During solar proton events (SPE) the ionisation is increasing especially at high latitudes. The SPE occuring during Forbush decreases of galactic CR, however, have rather complex effect on that (Usoskin et al. 2009).

18.1.2 The CR Precursors of Geoeffective Events

The CMEs have various size, geometry, speed and direction of motion with respect of the Earth (see http://cdaw.gsfc.nasa.gov/CME_list/) and they differ in geoeffectiveness (Gopalswamy et al. 2009).

Analysis of the CR measurements at the NM energies showed long time ago the existence of precursors before the arrival of an interplanetary shock to the Earth and before the onset of the Forbush decrease (Dorman 1963). Due to the high CR velocity, parallel mean free path λ_{par} and gyroradius, the information about precursory anisotropies related to the IMF inhomogenity, is transmitted fast to remote locations: intensity deficit of the CR can be observed up to the distance of 0.1 $\lambda_{par} \cos(\Phi)$, Φ - cone angle of IMF (Ruffolo 1999). Precursors to the Forbush decrease (FD) are proposed in the frame of the pitch-angle transport near oblique, plane-parallel shock. Assuming different values of the power-law index of magnetic turbulence, mean free path and decay length for typical primary energies to which the NM and muon detectors (MD) are sensitive. The loss cone precursors should be observed by NM ∼4 h prior to shock arrival, and by MD ∼15 h prior to shock arrival (Leerungnavarat et al. 2003).

Recently there have been reported several case and statistical type of studies on the precursors before the geomagnetic storms based on the CR anisotropy or specific features of the counting rate variability. The muon detectors (MD) are used for multidirectional measurements. The MD at Sao Martinho, Brazil, showed that subtracting contribution from the diurnal anisotropy determined by the Global Muon Detector Network (GMDN), the clear signatures of the precursor before the storm on December 14, 2006, were found (Fushishita et al. 2009). The loss cone precursor (deficit of the CR flux at small pitch angles) appeared

only ~6.6 h after the CME eruption on the Sun, when the interplanetary shock was expected to be located 0.2 AU from the Sun.

On the September 2005 the Forbush decrease was investigated and a clear modulation in about 8-h periodicity was emerging from the pre-Forbush subsets. The analyzed case study suggests that the CR datasets, containing seven days of data with 5-min time resolution, can give a signal for interplanetary storms approaching the Earth up to 9 hours before the onset of the FD-main phase at two NMs with different cutoff rigidities (Diego and Storini 2009).

New muon measurements were reported. Data from a large muon track detector – the hodoscope URAGAN (surface 34 m^2) around the heliospheric disturbances in 2007–2008 were analyzed. Each track was reconstructed with accuracy $< 1°$. Among 63 events, when URAGAN data existed, in 53 events (84%) disturbances of anisotropy vector had been observed. Although the distribution of time differences of perturbation between the ACE and the URAGAN were rather wide, the mean value of the onset time of perturbation by the two measurements was -13.6 ± 2.6 h (Timashkov et al. 2009).

The statistical study of CR precursors in 2001–2007 before different storms using the Global Muon Detector Network (GMDN) was done in the paper Da Silva et al. (2009). The storms were divided into three groups, namely the super storms (Dst< -250 nT); the intense storms (-250 nT $<$Dst< -100 nT); and the moderate storms (-100 nT $<$Dst< -50 nT). The percentage of the events accompanied by the precursors prior to the SSC increases with increasing peak Dst is: 15% of MSs, 30% of ISs and 86% of SSs were accompanied by CR precursors observed on average 7.2 h in advance of the SSC.

18.2 Using Magnetospheric Filter for the Energy Spectra of Accelerated Particles

Measurements within the magnetosphere can provide information about the solar and/or interplanetary acceleration of particles by using the geomagnetic field filter on charged particles and no effect on high energy photons and neutrons.

18.2.1 Charged Particles, Low Orbits

Having large geometrical factor for energetic particles measured at low, nearly polar orbiting satellites, the arrival of solar flare particles can be checked according to its boundary position and the flux at four segments of trajectory per one orbit. The CORONAS-F was a low altitude satellite (detailed description of the complex of measurements can be found in the paper Kuznetsov 2008) and one of the devices, namely SONG (described e.g. in Kuznetsov et al. 2004), had such possibility.

Checking value of proton flux at different L shells (4 times per orbit at selected Ls from 1.75 to 3) and assuming the simple shape of energy spectra of the type $J(>E) = J_0 E^{-\gamma}$, the spectra in Fig. 18.1 was obtained (Kuznetsov et al. 2007) and compared with the NMs (Vashenyuk et al. 2005; Miroshnichenko et al. 2005).

Recently the PAMELA experiment provided important information on the energy spectra of the SEP during the GLE on December 13, 2006. Combining the low energy measurements by the GOES (3 channels covering 30–500 MeV), three energy channels by the PAMELA (from 0.1 to 1 GeV) and NM data, the authors obtained the time evolution of the fit of spectra over long time period (De Simone et al. 2009a).
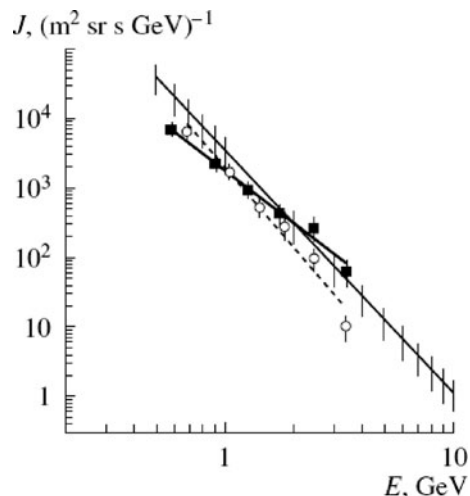

Fig. 18.1 Energy spectra of SEP on October 28, 2003 at 1,142–1,146 UT evening sector (*black squares*) and at 1,204–1,209 UT morning sector (*circles*) (Kuznetsov et al. 2007). Comparison with NM data (line >400 MeV) according to (Vashenyuk et al. 2005; Miroshnichenko et al. 2005)

For practical purposes the position of penetration boundary of the SEP was fitted from large amount of observations during different geomagnetic activity levels (Smart et al. 2006; Smart and Shea et al. 2009).

However, the position of the boundary of the SEP penetration to low orbits was not known exactly for the given geomagnetic activity level. The large spread of magnetic latitude at fixed Kp and Dst is illustrating that situation in the Fig. 18.2.

The boundary position during the penetration of the SEP on low orbits had rather complicated character especially during strong geomagnetic events. One of
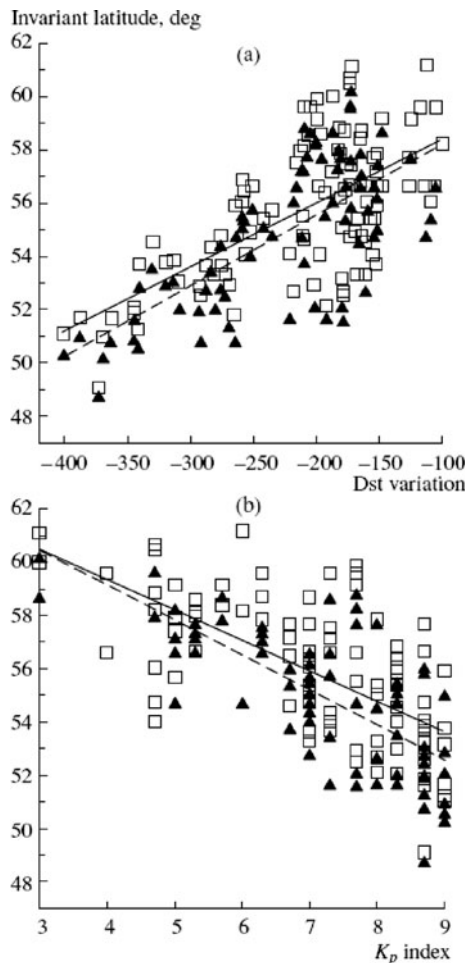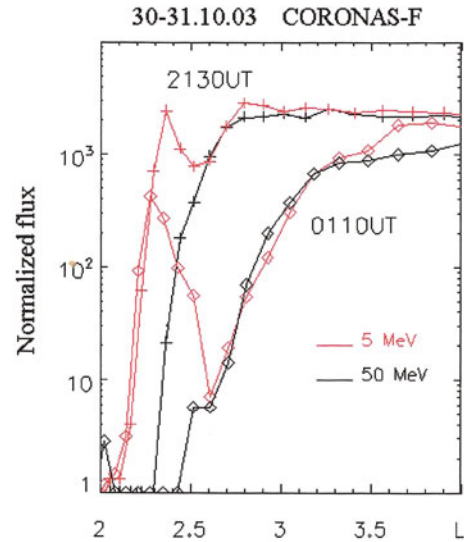
Fig. 18.3 Solar protons with energy 1–5 MeV might be trapped, creating temporary solar CR belts on $L = 2 - 3$ or providing additional flux to the previously existed population. This trapping action is observed as a double boundary effect in the Coronas-F measurements. Double boundary effect of 1–5 MeV protons is seen during the magnetic storm recovery phase, 30–31 October, 2003. The *dotted lines* indicate the penetration boundary of the 50–90 MeV protons. The *solid lines* indicate the penetration boundary of 1–5 MeV protons. (Lazutin et al. 2009)

specific features which had not been understood quite well was the double structure of the boundary position, This is shown in Fig. 18.3. Value of L at given position during the storms depends on the geomagnetic field model used.

Two more questions obtained from the observations remain not understood well, namely (a) 1–100 MeV SEP penetrate into the magnetosphere to lower latitudes as deep as it is not allowed by any magnetic field models, and (b) during some strong magnetic storms penetration boundaries coincide for wide energy range in comparison with normal (expected) penetration structure. This is seen from the Fig. 18.4.

Fig. 18.2 Dependences of the SEP penetration boundaries on (**a**) Dst and (**b**) Kp in the evening and night MLT sectors: invariant latitudes of the penetration boundaries for protons (*squares*) 1–5 and (*triangles*) 50–90 MeV and linear regression for (1–5)-MeV and (50–90)-MeV protons (*solid* and *dashed lines*, respectively) CORONAS-F. Interval 2001–2005. (Myagkova et al. 2009)

18.2.2 Neutral High Energy Emissions

The measurements of high energy photons not affected by geomagnetic field provide important information about the timing of proton acceleration in solar flares. Clear increase in the energy spectra of photons at energy 50–100 MeV, associated with π^o decay was
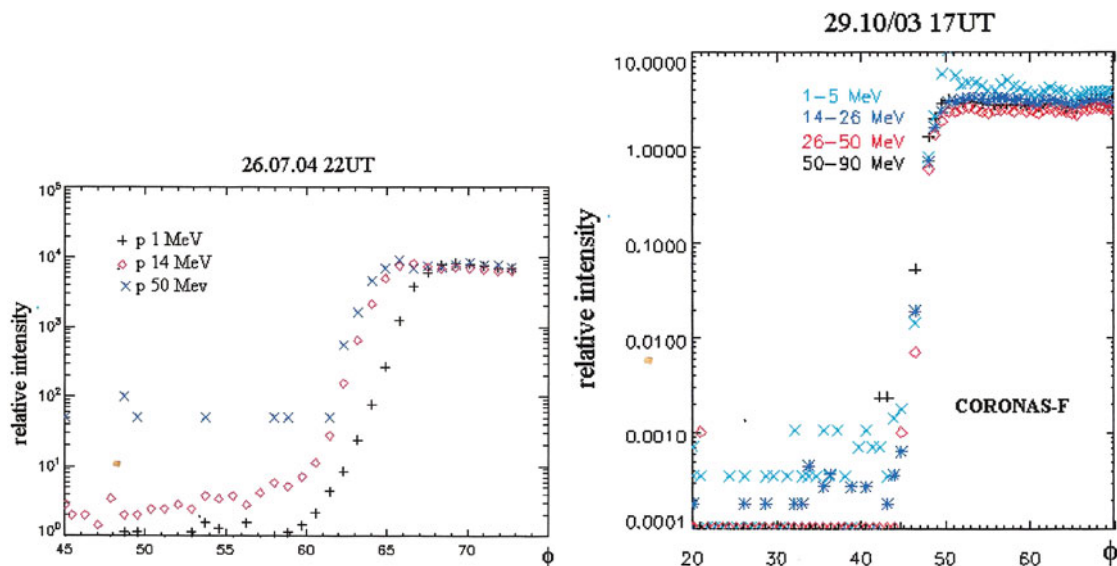
Fig. 18.4 While the boundary position during the event on July 26, 2004 was organized acording to the kinetic energy of protons (*left*), it was practically coinciding for the wide energy range in the strong geomagnetic disturbance on October 29, 2003. It is not clear: was it created by some special "transparency" of the magnetospheric boundary during strong magnetic storms or was it a consequence of some changes of the magnetic field structure of the inner magnetosphere?

Table 18.1 From (Kurt et al. 2009). The time onset of pion-decay gamma rays and the flux observed by the SONG on the CORONAS-F during strong solar flares for the period July 2001–January 2005

Date	Location/importance	Onset of π-decay γ emission, UT	γ-ray flux at 100 MeV, $[\text{MeV}^{-1}\text{cm}^{-2}\text{s}^{-1}]$	Particles
25 August 2001	S17E34, 3B/X5.3	16:30:16±2 s	7.3×10^{-4}	n
28 October 2003	S16E08, 4B/X17.2	11:03:51±2 s	6.8×10^{-3}	GLE65, n
04 November 2003	S19W83, X28.9	19:42:38±4 s	1.0×10^{-3}	n
20 January 2005	N14W61, 3B/X7.1	06:45:34±4 s	3.6×10^{-3}	GLE69

reported during some flares (Kurt et al. 2009). It indicated the exact time of energetic proton appearance in the solar atmosphere. This allows to compare the proton acceleration time with the start time of the GLE recorded by the ground NMs, and to calculate the time interval when the GLE particle escaped from the corona. It is shown for the four large flares observed by the SONG instrument on the CORONAS-F in Table 18.1.

18.3 Transmissivity Function and Albedo Cosmic Rays

The only possibility to obtain predictions of cosmic ray transmissivity through the magnetosphere is numerical tracing of particle motion in the given geomagnetic field model. The equation describing the particle motion in a static magnetic field leads to the system of 6 linear differential equations with unknown values (position, velocity vector) which is usually solved numerically (e.g. McCracken et al. 1965; Bobik 2001, among the others). The review of the progress of the 50 years trajectory calculation can be found in the paper (Smart et al. 2009). For the trajectory computations with the step dR summarized over larger rigidity interval DR, the useful approach is the transmissivity function TF(R,DR) – the probability that a particle of the rigidity (R,R+DR) can access the given point in the model field (Kudela and Usoskin 2004). Similar concept was introduced earlier – the cutoff probability (Heinrich and Spill 1979).

The application of the TF was used e.g. to estimate the contribution of the secondary CR population – the reentrant albedo particles at low earth orbits. The product of energy spectra of the galactic CR (CREME 96) and the TF for different bands of geomagnetic latitudes separated at the energies below the vertical cut-off the albedo particles from the measurements for the AMS experiment (Bobik et al. 2006) and recently also for PAMELA experiment (De Simone et al. 2009b).

18.4 Transmissivity of the CR During Geomagnetic Disturbances

For geomagnetically disturbed periods it was necessary to use the geomagnetic field models with external current systems. Out of them the three were used here for comparison of predictions of the TF for a strong geomagnetic storm when improvement of the transmissivity during large Dst depression has been observed as a combined effect – starting the Forbush decrease seen at low cut-off stations and the increase apparent at the middle and low latitude NMs. Depression of the *Dst* on November 20, 2003 to −475 nT was accompanied by strong increase of count rate on several NMs, especialy Rome (6.3 GV cutoff) and Athens (8.3 GV).

The three different geomagnetic field models, namely (i) Tsyganenko' 89 (Tsyganenko 1989); (ii) the Boberg model (Boberg et al. 1995) and (iii) Tsyganenko 2004 (Tsyganenko and Sitnov 2005) provided different TF functions for that period by trajectory computations for a middle latitude station (Fig.18.5).

The asymptotic directions for acceptance of the CR were similar for the three models before the storm. However, for the period of the minimum Dst, the structure of asymptotics was significantly different for different models. The third difference was in comparison of time of minimum cut-off rigidity (time of peak of the CR during the storm). For this particular case the better correspondence with measurements had been provided by the Tsyganenko 2004 model than by the other two. However, for another storm, namely November 7–8, 2004, it was not the case and the Boberg model (Boberg et al. 1995) including the Dst provided better alignment with maximum CR intensity than the Tsyganenko 2004 model. More details on comparison of different models with the CR is e.g. in the papers
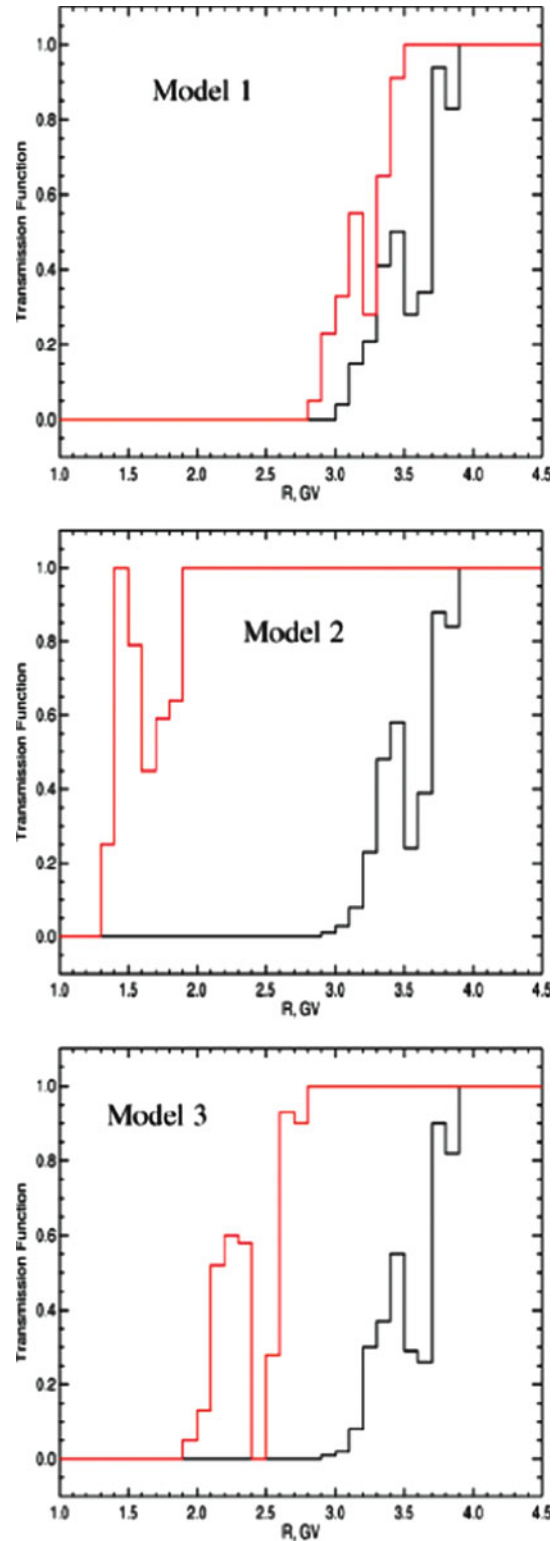

Fig. 18.5 TF (for vertical direction) for Lomnický Štít before the onset of the storm (November 20, 2003, 02 UT, *black*) and during the *Dst* minimum (19 UT, *red*) for three models. Adopted from (Kudela et al. 2008)

Kudela et al. (2008); Tyasto et al. (2008) among the others.

How to check correctly the validity of geomagnetic field models by the CR during the geomagnetic storms? It has to be assumed there are two effects superimposed during the geomagnetic storm, namely (i) the pure anisotropy of the CR in interplanetary medium during the CME propagation and "seen" by the CR coming to the magnetosphere, and (ii) the reconstruction of asymptotic directions; of the transmissivity and timing of the cut-off depression due to the changes of external current systems in the magnetosphere during disturbances. Thus, it is necessary to have an independent estimate of the interplanetary anisotropy if middle and low latitude NMs are used for checking the validity of the field models existing. There may be useful an approach from both sides of the primary spectra. The Spaceship Earth (Bieber and Evenson 1995), the ring of the NMs at high latitudes providing the anisotropy at low energies (not strongly affected by magnetospheric disturbance with asymptotic directions in narrow interval of longitudes, close to the ecliptic), and not strongly changing the system of asymptotics due to the magnetosphere's reconstruction (below the atmospheric cut-off) may serve as a potential estimate for the interplanetary CR anisotropy at low energies. On the other hand, the network of muon directional telescopes (Munakata et al. 2000) studies anisotropy at energies above NM ($\sim$50 GeV), not strongly affected by the changes in the magnetosphere. This may serve as an estimate of the anisotropy at high energies. If consistent picture of anisotropies in interplanetary space at low and high energies is obtained for a geomagnetic storm, and the estimate of anisotropy at "middle energies" is estimated, the validity of various geomagnetic field models during geomagnetic storms can be done with using the world wide network of the NMs as well as with new instruments as e.g. Chilingarian et al. (2009). In addition, energization of electrons to relativistic energies during the substorms puts also constraints on magnetospheric topology and on the geomagnetic field models (Antonova et al. 2009; Antonova 2009).

18.5 Summary

For radiation hazard events the alerts from both single point measurements of the CR at different energies (South Pole) and the NM network progressed in recent years – alerts constructed earlier than those from the satellites (for GLEs), are providing estimation of the fluence and peak intensity. High potential of electron measurements is stressed. New space instruments for that are in preparation (e.g. Grimani and Fabi 2009).

Progress in geoeffective events precursor studies is reported, namely new case and statistical studies, especially at high energies (GMDN), and the new instruments (e.g. URAGAN hodoscope) are showing potential possibilities of the alert. The CMEs have various size, geometry, speed and direction of motion with respect of the Earth and they differ in geoeffectiveness. The problem with using only CR signatures remains in the large variability of precursory timing from the anisotropy onset to the onset of geomagnetic storm. Anisotropy depends on geometry, velocity and direction of CME motion, and on magnetic field structure. Thus information from the CR can be used as an additional parameter for the forecast of geoeffective events.

Energy spectra of the SEP at low nearly polar orbits were obtained (e.g. CORONAS-F, PAMELA) based on the knowledge of cut-offs. Detailed empirical models of cut-offs (with parameter Kp) exist. There is, however, observed large variability of the boundary position for the geomagnetic activity given by the Kp and Dst only. Double boundary with the trapping of protons was observed during the strong storms. Boundary of penetration and reconfiguration of magnetospheric fluxes during the storms may serve as a source for verification of geomagnetic field models (also for the trapped populations when fluxes are described by the adiabatic invariants). Some puzzles remain: e.g. during strong storms the penetration boundaries are almost identical in wide energy range of protons. High energy gamma rays and neutrons measured at low orbits provide unique additional information about the time of acceleration of protons.

During strong geomagnetic storms at the NM energies the different field models provide different TF, asymptotic directions and timing of the CR variations. An "overlap" of interplanetary anisotropy and the changes in conditions of particle access during the geomagnetic disturbances remains a problem for testing the validity of geomagnetic field models during these events by the worldwide network of the NMs. Comparison of interplanetary anisotropy estimates at high energies (by GMDN) and at the low ones (e.g. Spaceship Earth) is needed, if middle and low latitude NMs are used for the geomagnetic field model verifications.

References

Anashin V, Belov A, Eroshenko E et al (2009) The ALERT signal of ground level enhancements of solar cosmic rays: physics basis, the ways of realization and development. Proceedings of the 31st ICRC, Lodz, icrc1104, 2009

Antonova EE, Kirpichev IP, Stepanova MV et al (2009) Topology of the high latitude magnetosphere during large magnetic storms and the main mechanisms of relativistic electron acceleration, Adv Space Res 43(4, 16):628–633

Antonova EE (2009) Regular and turbulent mechanisms of relativistic electron acceleration in the magnetosphere of the Earth: theoretical treatment and results of experimental observations. Proceedings of the 21st ECRS, Kosice, p 17–26

Bieber JW, Evenson P (1995) Spaceship Earth - an optimized network of neutron monitors. Proceedings of the 24th ICRC, Rome, vol 4, pp 1316–1319

Bieber JW et al (2006) AOGS 3rd Annual Meeting, Singapore, 2006

Bazilevskaya GA, Usoskin IG, Flckiger EO et al (2008) Cosmic ray induced ion production in the atmosphere. Space Sci Rev 137:149–173

Boberg PR, Tylka AJ, Adams JH Jr et al (1995) Geomagnetic transmission of solar energetic protons during the geomagnetic disturbance of October 1989. Geophys Res Lett 22(9):1133–1136

Bobik P (2001) PhD Thesis, P.J. Safarik University, Kosice

Bobik P, Boella G, Boschini MJ et al (2006) Magnetospheric transmission function approach to disentangle primary from secondary cosmic ray fluxes in the penumbra region. J Geophys Res 111(A5):A05205 10.1029/2005JA011235

Chilingarian A, Hovsepyan G, Arakelyan K et al (2009) Space environmental viewing and analysis network (SEVAN). Earth, Moon Planets 104(1–4):195–210

Da Silva MR, Dal Lago A, Gonzalez WD et al (2009) Global muon detector network observing geomagnetic storm's precursor since March 2001. In: Proceedings of the 31st ICRC, Lodz, icrc0739, 2009

De Simone N, Adriani O, Barbarino GC et al (2009a) Study of protons of solar origin in the events of 13 and 14 December 2006 with Pamela detector. In: Proceedings of the 31st ICRC, Lodz, icrc0794, 2009

De Simone N, Adriani, O, Barbarino GC et al (2009b) Comparison of models and measurements of protons of trapped and secondary origin with PAMELA experiment. In: Proceedings of the 31st ICRC, Lodz, icrc0255, 2009

Diego P, Storini M (2009) Modulation signatures on cosmic-ray periodicities before a forbush decrease. In: Proc. 31st ICRC, Lodz, icrc0044, 2009

Dorman LI (1963) Geophysical and astrophysical aspects of cosmic rays. North-Holland, New York, NY

Dorman L (2009) Cosmic Rays in magnetospheres of the Earth and other planets. Lightning Source UK Ltd, Milton Keynes Springer

Flückiger EO (1982) Rep. No. AFGL-TR-82-0177

Fushishita A, Munakata K, Miyasaka E et al (2009) Precursors of the Forbush decrease on December 14, 2006 observed with the Global Muon Detector Network (GMDN). In: Proceedings of the 31st ICRC, Lodz, icrc0502, 2009

Gopalswamy N, Maekelae P, Xie H et al (2009) CME interactions with coronal holes and their interplanetary consequences. J Geophys Res 114:A00A22

Grimani C, Fabi M (2009) Short-term forecasting of solar energetic ions on board LISA. Proceedings of the 31st ICRC, Lodz, icrc0255

Heinrich W, Spill A (1979) Geomagnetic shielding of cosmic rays for different satellite orbits. J Geophys Res 84(A8):4401–4404

Kassovicova J, Kudela K (1998) On the computations of cosmic ray trajectories in the geomagnetic field, Preprint IEP SAS, Kosice, 1998, pp 1–12

Kudela K (2009) Cosmic rays and space weather: direct and indirect relations. In: D'Olivo JC, Medina-Tanco G, Valdés-Galicia JF (eds) Proceedings of the 30th international cosmic ray conference, Rogelio Caballero. Universidad Nacional Autonóma de México, Mexico City, Mexico, vol 6, pp 195–208

Kudela K, Bucik R, Bobik P (2008) On transmissivity of low energy cosmic rays in disturbed magnetosphere. Adv Space Res 42:1300–1306

Kudela K, Storini M, Hofer MY, Belov A (2000) Cosmic rays in relation to space weather. Space Sci Rev 93(1–2):153–174

Kudela K, Usoskin IG (2004) On magnetospheric transmissivity of cosmic rays. Czech. J. Phys. 54, 239–254

Kurt VG, Yushkov BY, Kudela K et al (2009) High-energy gamma-ray emission of solar flares as an indicator of acceleration of high-energy protons. In: Proceedings of the 31st ICRC, Lodz, icrc0589, 2009

Kuwabara T, Bieber JW, Clem J et al (2006) Development of a ground level enhancement alarm system based upon neutron monitors. Space Weather 4, 10, S10001, Oct 11, 2006

Kuznetsov VD (2008) Observations of the Sun-Earth system within the CORONAS-F mission (July 31, 2001 to December 6, 2005). J Atmos Solar-Terr Phys 70(2–4):234–240

Kuznetsov SN, Kudela K, Myagkova IN et al (2004) First experience with SONGM measurements on board CORONAS-F satellite. Indian J Radio Space Phys 33(6): 353–357

Kuznetsov SN, Yushkov BY, Kudela K (2007) Measurement of the spectrum of relativistic protons from solar flares on October 28 and November 2, 2003 onboard The CORONAS-F satellite. Cosmic Res 45(4) 373–375

Lazutin LL, Kuznetsov SN, Panasyuk YM (2009) Solar cosmic rays as a source of the temporary inner radiation belts. Adv Space Res 44:371–375

Leerungnavarat K, Ruffolo D, Bieber JW (2003) Loss cone precursors to Forbush decreases and advance warning of space weather effects. Astrophys J 593(1 Pt 1):587–596

Mavromichalaki E, Souvatzoglou G, Sarlanis C et al (2009) Using the real-time NeutronMonitorDatabase to establish an Alert signal. In: Proceedings of the 31st ICRC, Lodz, icrc1381, 2009

McCracken KG, Rao UR, Fowler BC, Shea MA, Smart DF (1965) IQSY Instruction manual No 10, Cosmic Ray Tables (Asymptotic directions, variational coefficients and cut-off rigidities), Issued by IQSY Committee, 6 Cornwall Terrace, London NW1, 183 pp, May 1965

Miroshnichenko LI, Klein K-L, Trottet G et al (2005) Relativistic Nucleon and Electron Production in the 2003 October 28 Solar Event, J Geophys Res vol 110:A09S08. doi:10.1029/2004JA010936

Munakata K, Bieber JW, Yasue S-I et al (2000) Precursors of geomagnetic storms observed by the muon detector network. J Geophys Res 105(27):457

Myagkova IN, Bogomolov AV, Yushkov BY et al (2009) Study of the extreme location of the penetration boundary of solar energetic particles (protons) into the Earth's magnetosphere during the magnetic storms in 2001–2005. Bull Russian Acad Sci: Phys 73(3):322–324

Posner A (2007) Up to 1-hour forecasting of radiation hazards from solar energetic ion events with relativistic electrons. Space Weather 5(5):S05001

Ruffolo D (1999) Transport and acceleration of energetic charged particles near an oblique shock. Astrophys J 515(2):787–800

Smart DF, Shea MA (2009) Fifty years of progress in geomagnetic cutoff rigidity determinations. Advances in Space Research, accepted, online ScienceDirect

Smart DF, Shea MA, Tylka AJ (2006) A geomagnetic cutoff rigidity interpolation tool: accuracy verification and application to space weather. Adv Space Res 37:1206–1217

Stozhkov YI, Svirzhevsky NS, Bazilevskaya GA et al (2007) Fluxes of cosmic rays in the maximum of absorption curve in the atmosphere and at the atmosphere boundary (1957–2007). Preprint FIAN, pp 77

Timashkov DA, Barbashina NS, Chernov DV et al (2009) Analysis of heliospheric disturbances during solar minimum using data of muon hodoscope URAGAN. In: Proceedings of the 31st ICRC, Lodz, icrc0891, 2009

Tsyganenko NA (1989) A magnetospheric magnetic field model with a warped tail current sheet. Planet Space Sci 37(1):5–20

Tsyganenko NA, Sitnov MI (2005) Modelling the dynamics of the inner magnetosphere during strong geomagnetic storms. J Geophys Res 110:A03208. doi:10.129/2004JA010798

Tyasto MI, Danilova OA, Dorman LI et al (2008) On the possibility to check the magnetosphere's model by CR: the strong geomagnetic storm in November 2003. Adv Space Res 42:1556–1563

Su Yeon Oh, Bieber JW, Clem J et al (2009) Neutron monitor forecasting of radiation storm intensity. In: Proceedings of the 31st ICRC, Lodz, icrc0602, 2009

Usoskin IG, Tylka AJ, Kovaltsov GA et al (2009) Ionization effect of strong solar particle events: low-middle atmosphere. In: Proceedings of the 31st ICRC, Lodz, icrc0162, 2009

Vashenyuk EV, Miroshnichenko LI, Balabin YV et al (2005) Dynamics of relativistic SCR in the events of October–November 2003. Izv Akad Nauk Ser Fiz 69(6):808–811 http://cdaw.gsfc.nasa.gov/CMElist/